Unusual Hydration Properties of C16:0 Sulfatide Bilayer Membranes

Kumkum Saxena,[†‡] Richard I. Duclos Jr.,[†] Pavanaram K. Sripada,[†] and G. Graham Shipley[†‡]

Departments of [†]Biophysics and [‡]Biochemistry, Center for Advanced Biomedical Research, Boston University School of Medicine, Boston, Massachusetts 02118 USA

ABSTRACT   After deacylation of bovine brain sulfatide under mild alkaline conditions and reacylation using palmitoyl chloride (Koshy and Boggs, 1983, *Chem. Phys. Lipids.* 34:41–53), the anionic glycosphingolipid *N*-palmitoyl galactosulfatide (C16:0-GalSulf) has been synthesized. By differential scanning calorimetry (DSC), anhydrous C16:0-GalSulf exhibits an endothermic transition, $T_M = 93°C$ ($\Delta H = 5.5$ kcal/mol C16:0-GalSulf) on heating. With increasing hydration (50 mM sodium phosphate buffer, pH 7.0; 50 mM NaCl), T_M decreases, reaching a limiting value of 49°C ($\Delta H = 8.2$ kcal/mol C16:0-GalSulf) at 20 wt% buffer. X-ray diffraction data have been recorded over the hydration range 0–62% at temperatures below (20°C) and above (60°C) T_M. At 20°C, sharp wide-angle reflections at $\sim 1/4.4$ Å^{-1}, $\sim 1/4.1$ Å^{-1}, and $\sim 1/3.8$ Å^{-1} indicate the presence of an ordered-chain gel phase, whereas at 60°C a broad reflection at $1/4.5$ Å^{-1} characteristic of a melted-chain phase is observed. Lamellar diffraction patterns consistent with the presence of bilayer phases are observed at both temperatures. At 60°C, in the liquid-crystalline L_α phase, the bilayer periodicity increases with hydration, in both water and 100 mM Na$^+$ buffer. Interestingly, in the gel phase at 20°C, the bilayer periodicity ($d = 64$ Å) is insensitive to hydration (over the range 30–60 wt%) with either water or buffer. The continuous swelling behavior exhibited by the L_α bilayer phase of C16:0-GalSulf is typical of lipids bearing a net negative charge and confirms that the presence of 100 mM Na$^+$ is insufficient to shield the charge contributed by the sulfate group. In contrast, the lack of continuous swelling behavior of the bilayer gel phase of C16:0-GalSulf is unusual and resembles that of Na$^+$ soaps. Thus, presumably, alterations in the surface charge characteristics of the C16:0-GalSulf bilayer occur on hydrocarbon chain melting and lead to major changes in lipid hydration.

INTRODUCTION

Phospholipids, glycosphingolipids (GSLs), and cholesterol are the major constituents of the lipid bilayer matrix in which a variety of membrane proteins (enzymes, receptors, channels, etc.) are arranged. In general, these lipids contribute to the structural organization and stability of the membrane bilayer, but in addition, individual lipids have specific functions. The latter include the second messenger signaling properties resulting from the hydrolysis of phospholipids such as phosphatidylcholine, phosphatidylinositol, and sphingomyelin (Exton, 1994; Nishizuka, 1992; Berridge, 1993; Hannun, 1994). The functions of GSLs include their role in cell-cell communication (Hakomori and Igarashi, 1995) and their activity as cell surface receptors for hormones, bacterial toxins, and viruses (van den Berg et al., 1992; Fishman et al., 1993; Harouse et al., 1991). Recently it has been shown that GSLs (together with sphingomyelins and cholesterol) concentrate in detergent-resistant domains of the plasma membrane; these GSL-rich domains are thought to be related to the membrane caveolae in which

some membrane receptors are located (Brown and London, 1998).

Even the simplest monoglycosyl GSLs (i.e., cerebrosides) are capable of binding complex ligands. For example, cerebrosides (particularly galactocerebroside) can act as a receptor for the human immunodeficiency virus 1 (HIV-1) in CD4-negative cell lines derived from the nervous system (Harouse et al., 1991). The sulfated galactocerebroside, galactosulfatide, has also shown to bind HIV (van den Berg et al., 1992). Furthermore, it has been well documented that sulfatides can bind to specific components of the extracellular matrix, such as laminin, von Willebrand factor, and thrombospondin (Roberts, 1986; Ginsburg and Roberts, 1988); these sulfatide-matrix interactions occur with an affinity equivalent to that characteristic of receptor-ligand interactions and may play a role in cell adhesion processes. More recently it has been shown that sulfatides (and other sulfated GSLs) bind to selectins and could be involved in cell-cell interactions (for example, see Suzuki et al., 1993).

Our overall goal has been to define the structure and properties of different GSLs. Our studies have focused on 1) natural GSLs with heterogeneous fatty acyl chains (Curatolo et al., 1977; Ruocco and Shipley, 1986), 2) partially synthetic GSLs with controlled fatty acid composition but some variability in the sphingosine moiety (Ruocco et al., 1981; Reed and Shipley, 1987, 1989; Haas and Shipley, 1995), and, most recently, 3) totally synthetic GSLs, pure with respect to stereochemistry, chain, and sphingosine composition (Shah et al., 1995; Saxena et al., 1999, 2000). We hope to provide an assessment of the contributions of acyl chain structure (chain length, unsaturation, hydroxylation), sphingosine structure (chain length, unsaturation, hy-

droxylation), and, most importantly, oligosaccharide complexity (number of sugars, charge characteristics) to GSL structure, hydration, and properties.

For the single sugar cerebrosides, we have defined the properties of several galactocerebrosides differing in chain length and chain unsaturation (Ruocco et al., 1981; Reed and Shipley, 1987, 1989; Haas and Shipley, 1995) and compared the behavior of totally synthetic C16:0 galacto- and glucocerebrosides (Saxena et al., 1999). We have explored the structure and thermotropic and hydration properties of C16:0-galactocerebroside (C16:0-GalCer, *N*-palmitoyl galactocerebroside) (Ruocco et al., 1981; Ruocco and Shipley, 1983), as well as its interactions with phospholipids and cholesterol (Ruocco et al., 1981, 1983; Ruocco and Shipley, 1984). To investigate the effect of a charged sulfate group on cerebroside behavior, our initial studies described the structure and thermotropic properties of bovine brain sulfatide (Ruocco and Shipley, 1986). Differential scanning calorimetry (DSC) and x-ray diffraction showed that hydrated sulfatide dispersions undergo a complex chain-melting transition over the range 32–47°C. The low transition enthalpy and transition temperature of sulfatide compared to those of bovine brain cerebrosides (Curatolo, 1982) were attributed to the sulfate charge-mediated disruption of the hydrogen bonding network at the sugar-interface region of sulfatide (Ruocco and Shipley, 1986). X-ray diffraction studies of the liquid-crystalline phase of sulfatide at 75°C showed a bilayer structure over the hydration range16–50 wt % phosphate buffer (pH 7.4). The intrabilayer separation between galactosyl-3-sulfate groups, 48 Å, remains unchanged as the sulfatide bilayers swell continuously with the addition of phosphate buffer (Ruocco and Shipley, 1986). Thus, in contrast to the limited hydration properties of bilayers of neutral GSLs (specifically, cerebrosides; Reiss-Husson, 1967; Abrahamsson et al., 1972; Ruocco et al., 1981; Lynch et al., 1992), bilayers of sulfatide in their melted-chain liquid-crystalline L_α phase undergo continuous swelling due to the presence of the charged sulfate group.

Boggs et al. (1984) have used DSC to study the phase behavior of partially synthetic sulfatides containing different fatty acids (palmitic, stearic, lignoceric, D-2-hydroxy palmitic, and D-2-hydroxy stearic), in the presence of mono- and divalent cations. Both the nonhydroxy fatty acid (NFA) and hydroxy fatty acid (HFA) forms of sulfatide can occur in two different gel states, a metastable state and a lower entropy stable state. The phase behavior is more sensitive to the type and concentration of cation present than is the case with acidic phospholipids. The sensitivity of the transition temperature (T_M) to cation concentration is thought to reflect, in part, increased participation of the sulfatide in intermolecular hydrogen bonding interactions as the negative charge of the sulfate group is shielded by the presence of counterion (Boggs et al., 1984).

To compare directly the structural behavior of sulfatide with the previously studied C16:0-galactocerebroside (Ruocco et al., 1981; Saxena et al., 1999), we have synthesized the corresponding sulfatide, *N*-palmitoyl-galactosyl-3-sulfate (C16:0-GalSulf). In this paper we focus on the structure and properties of C16:0-GalSulf as revealed by DSC and x-ray diffraction. In particular, we have examined the hydration characteristics of C16:0-GalSulf in different phases.

MATERIALS AND METHODS

Synthesis

Commercial (Matreya, Pleasant Gap, PA) bovine brain sulfatides, which were determined to be mostly the 24:1 fatty acyl analog of the sphing-4-enine sphingosine base by fast atom bombardment mass spectrometry (FABMS) (negative mode), were hydrolyzed in alkaline 90:10 MeOH/H_2O as reported previously (Koshy and Boggs, 1982). Before chromatography, the free fatty acid by-product was mostly removed by the acetonitrile precipitation method (Marchesini et al., 1987). Silica gel 60 chromatography (60:25:4 CHCl$_3$/MeOH/H_2O) gave lysosulfatide that was homogeneous by thin-layer chromatography with both neutral (60:25:4 CHCl$_3$/MeOH/H_2O) and basic (60:25:4 CHCl$_3$/MeOH/aq NH$_4$OH) conditions. Visualization was by the charring method (Bitman and Wood, 1982), and duplicate plates demonstrated the product to be ninhydrin positive. The amorphous white solid melted above 100°C. The zwitterionic compound had a negligible positive specific rotation in CHCl$_3$/MeOH but a somewhat higher positive rotation in CHCl$_3$/MeOH/aq NH$_4$OH. The ^{1}H and ^{13}C NMR spectra of lysosulfatide were as reported (Taketomi et al., 1990). The IR (KBr) spectrum was identical to previously reported spectra (Nonaka et al., 1979; Koshy and Boggs, 1982). The FABMS (negative mode) spectrum showed the molecular ion at *m/z* 540 as previously reported (Taketomi et al., 1990).

The acylation of lysosulfatide to give semisynthetic sulfatide (*N*-palmitoyl-galactosylsphingosine I^3-sulfate, C16:0-GalSulf) with palmitoyl chloride was performed by the reported method (Koshy and Boggs, 1983). The crude product was first purified by the reported *O*-(diethylaminoethyl)cellulose ion-exchange chromatography method to remove palmitic acid and a small amount of an impurity that elutes just ahead of C16:0-GalSulf. Silica gel chromatography (60:25:4 CHCl$_3$/MeOH/aq NH$_4$OH) followed by micropore (0.5 μm polytetrafluoroethylene Teflon) filtration of the product solution (95:5 CHCl$_3$/MeOH) gave C16:0-GalSulf that was homogeneous by thin-layer chromatography under both neutral and basic conditions and identical to previous preparations of semisynthetic C16:0-GalSulf (Koshy and Boggs, 1983; Boggs et al., 1984, 1988a,b). The C16:0-GalSulf was an amorphous white solid that had a sharp melting point of 179–181°C. The specific rotation was $[\alpha]_D^{25}$ +5° (c 1.5, 60:25:4 CHCl$_3$/MeOH/aq NH$_4$OH). The ^{1}H and ^{13}C NMR spectra were as reported for synthetic C16:0-GalSulf (Marinier et al., 1997) and the related analog (Tanahashi et al., 1997). The IR (KBr) spectrum was identical to the spectrum reported by Koshy and Boggs (1983). The FABMS (negative mode) spectrum showed the molecular ion at *m/z* 778. The semisynthetic C16:0-GalSulf gave an acceptable elemental analysis for the 16:0 fatty acyl sphing-4-enine product as the ammonium salt monohydrate.

Differential scanning calorimetry

For anhydrous samples, lyophilized sulfatide (2–4 mg) was transferred directly into preweighed stainless steel DSC pans and hermetically sealed. For hydrated samples, appropriate volumes of buffer (50 mM sodium phosphate, pH 7.0; 50 mM NaCl) were added to the pans with a microsyringe before sealing. Heating and cooling scans over the temperature range

0–70°C were performed on a Perkin-Elmer (Norwalk, CT) DSC-2 or DSC-7 calorimeter. Heating and cooling rates ranged from 0.1 to 40°C. Peak maxima were taken as the transition temperature (T_M), and transition enthalpies (ΔH) were determined from the area under the transition peak by comparison with that of a known standard (gallium).

X-ray diffraction

Hydrated samples for x-ray diffraction were prepared by weighing anhydrous C16:0-GalSulf into thin-walled capillary tubes (internal diameter 1 mm), followed by gravimetric addition of distilled, deionized water or buffer (50 mM sodium phosphate, pH 7.0; 50 mM NaCl). Sample tubes were covered with parafilm, centrifuged at room temperature for ~2 min, then flame-sealed. The dispersions were homogenized through the cycle centrifugation–sample inversion–centrifugation at a temperature above the transition temperature. X-ray diffraction patterns were recorded with photographic film, using nickel-filtered CuK$_\alpha$ x-rays from an Elliot GX-6 rotating anode generator (Elliot Automation, Borehamwood, UK). X-rays were focused into a point source with either toroidal mirror (Elliot, 1965) or double mirror (Franks, 1958) optics. Temperature-dependent x-ray diffraction data were also recorded with a position-sensitive linear detector (Tennelec, Oak Ridge, TN) and associated electronics (Tracor Northern, Middleton, WI). Nickel-filtered CuK$_\alpha$ x-rays from a microfocus generator (Jarrel-Ash, Waltham, MA) were line focused with a single mirror and collimated with the slit optical system of a Luzzati-Baro camera (E^{TS} Beaudoin, Paris, France).

RESULTS

Differential scanning calorimetry

The calorimetric behavior of C16:0-GalSulf in 79.6 wt% buffer (50 mM sodium phosphate buffer, pH 7.0; 50 mM NaCl) is shown in Fig. 1. After equilibration by repeated heating and cooling cycles, the initial heating scan at 5°C/ min shows an endothermic transition with a peak maximum at 48.7°C (Fig. 1 *a*); a very broad transition is also observed at 30–45°C. The combined enthalpy of the broad pretransition and the sharp transition is 8.0 kcal/mol C16:0-GalSulf. On cooling from 60°C at 5°C/min, C16:0-GalSulf exhibits essentially reversible behavior, with little or no supercooling (cf. Fig. 1, *a* and *b*). The total enthalpy associated with the cooling transitions is 8.1 kcal/mol C16:0-GalSulf. As shown in Fig. 1 *c*, the DSC heating scan (5°C/min) performed immediately after completion of the cooling scan is essentially identical to that shown in Fig. 1 *a*. Further heating and cooling scans at 5°C/min exhibit behavior identical to that shown in Fig. 1. Thus hydrated C16:0-GalSulf exhibits reversible thermotropic behavior.

DSC heating scans (5°C/min) of C16:0-GalSulf as a function of hydration are shown in Fig. 2. On heating, anhydrous C16:0-GalSulf undergoes a sharp endothermic transition at 93°C, $\Delta H = 5.4$ kcal/mol (Fig. 2 *a*). With increasing hydration, the transition shifts progressively to lower temperatures. At 7.9 wt% buffer, C16:0-GalSulf shows a broad transition with a peak maximum at 68°C (Fig. 2 *b*); at 19.3 wt% buffer, a broad (25–65°C) complex transition with peak maxima at 48°C and 54°C is observed (Fig. 2 *c*). Above 19 wt% buffer, the transition temperature
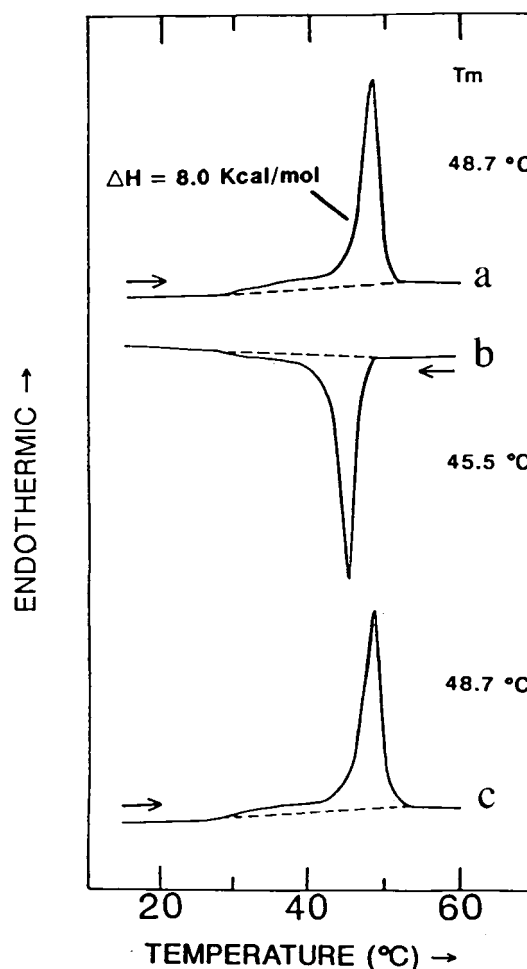

FIGURE 1 Reversible DSC behavior of hydrated C16:0-GalSulf (79.6 wt% buffer; 50 mM sodium phosphate, pH 7.0; 50 mM NaCl). (*a*) Initial heating scan after equilibration. (*b*) Cooling scan. (*c*) Heating scan, immediately after cooling. Heating/cooling rates, 5°C/min.

remains constant at 49°C (Fig. 2, *d–f*); a broad low-temperature transition precedes the major endothermic transition at all hydrations (see Fig. 2. *b–f*). The effect of hydration on the transition temperatures, enthalpies, and entropies of hydrated C16:0-GalSulf is shown in Fig. 3. Between 0 and 19 wt% buffer the transition temperature decreases from 93°C to its limiting value, 49°C; over the same hydration range, the transition enthalpy ΔH increases from 5.4 to 8 kcal/mol, and the transition entropy ΔS increases from 58 to 165 cal/mol/°C.

X-ray diffraction

X-ray diffraction patterns of C16:0-GalSulf at different hydrations in both buffer (50 mM sodium phosphate, pH 7.0; 50 mM NaCl) and water were recorded at temperatures below and above the appropriate transition temperature. For anhydrous C16:0-GalSulf at 20°C, six lamellar reflections
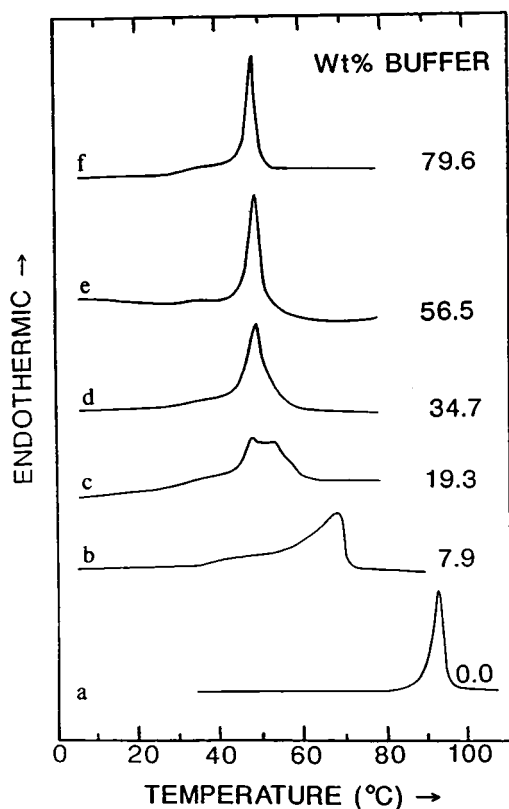
FIGURE 2 Differential scanning calorimetry of C16:0-GalSulf as a function of hydration (buffer; 50 mM sodium phosphate, pH 7.0; 50 mM NaCl). (*a*) 0.0. (*b*) 7.9. (*c*) 19.3. (*d*) 34.7. (*e*) 56.5. (*f*) 79.6 wt% buffer. Heating rate, 5°C/min.

FIGURE 3 (*A*) Effect of hydration on the transition temperature T_M (*A*), transition enthalpy ΔH (*B*), and transition entropy ΔS (*B*) of C16:0-GalSulf. Aqueous dispersions of C16:0-GalSulf were prepared in buffer (50 mM sodium phosphate buffer, pH 7.0; 50 mM NaCl).

corresponding to a periodicity $d = 58$ Å were observed together with a single, strong wide-angle reflection of 1/4.19 Å^{-1} (data not shown). At 95°C, above the transition temperature at 92.7°C, strong first- and second-order lamellar reflections are observed, corresponding to a reduced bilayer periodicity, $d = 43.6$ Å (data not shown); a diffuse wide-angle reflection of 1/4.5 Å^{-1} is characteristic of disordered hydrocarbon chain packing (Luzzati, 1968).

Representative x-ray diffraction patterns of hydrated C16:0-GalSulf in buffer and water are shown in Figs. 4 and 5, respectively. X-ray diffraction patterns are shown in Fig. 4 for C16:0-GalSulf at 31 wt% buffer. At 20°C, six low-angle lamellar reflections are observed, corresponding to a bilayer periodicity $d = 63.8$ Å (Fig. 4 *A*). Interestingly, three reflections at 1/4.36, 1/4.10, and 1/3.80 Å^{-1} are observed in the wide-angle region (see Fig. 4 *A, inset*) indicative of an ordered chain packing mode in the low-temperature gel phase. At 60°C, above the transition temperature, six lamellar reflections, corresponding to a bilayer periodicity $d = 62.1$ Å, are observed (Fig. 4 *B*); the broad wide-angle reflection at 1/4.5 Å^{-1} (Fig. 4 *B, inset*) is indicative of chain melting. X-ray diffraction data (not

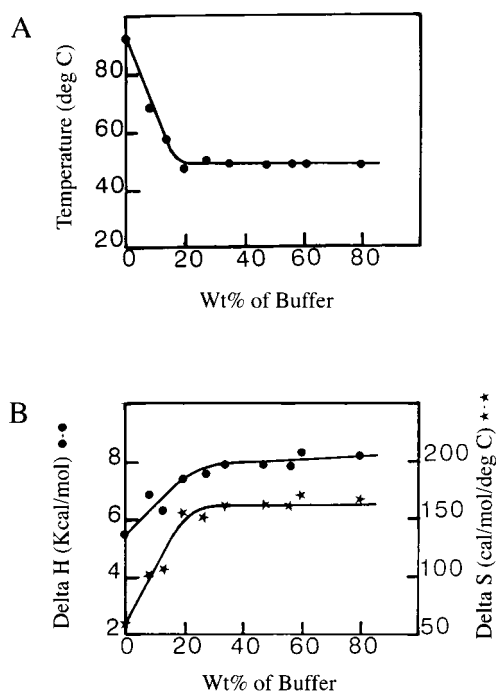shown) were also recorded from C16:0-GalSulf at 15, 45, and 62 wt% buffer.

As an example of the hydration behavior of C16:0-GalSulf in water, x-ray diffraction patterns for C16:0-GalSulf at 60 wt% water are shown in Fig. 5. At 20°C, below the transition temperature at 49°C, six low-angle lamellar reflections are observed, corresponding to a bilayer periodicity $d = 63.7$ Å (Fig. 5 *A*). The wide-angle region shows three reflections at 1/4.39, 1/4.10, and 1/3.80 Å^{-1} (see Fig. 5 *A, inset*). Despite the difference in hydration level, this diffraction pattern is essentially identical to that of C16:0-GalSulf at 31 wt% buffer described above. At 60°C, above the chain-melting transition, four lamellar reflections corresponding to a significantly increased bilayer periodicity, $d = 95.4$ Å, are observed (Fig. 5 *B*); a diffuse wide-angle reflection at 1/4.5 Å^{-1} (Fig. 5 *B, inset*) is indicative of chain melting. The significant increase in bilayer periodicity observed above the chain-melting transition indicates that C16:0-GalSulf hydrates much more readily in the liquid-crystal bilayer phase than in the low-temperature bilayer gel phase.

X-ray diffraction patterns of C16:0-GalSulf at 60 wt% water were also recorded as a function of temperature with a linear position-sensitive detector (Fig. 6). Below 48°C, the low-angle region shows a strong first-order reflection and weaker third- and fourth-order lamellar reflections corresponding to a bilayer periodicity $d \approx 63$ Å; the second-order

FIGURE 4 X-ray diffraction patterns of hydrated (31 wt%) C16:0-GalSulf in buffer (50 mM sodium phosphate, pH 7.0; 50 mM NaCl) recorded with a Franks camera at (*A*) 20°C (below the chain-melting transition) and (*B*) 60°C (above the chain-melting transition). Corresponding x-ray diffraction patterns recorded with a toroidal camera are shown as insets (*left*, 20°C; *right*, 60°C).
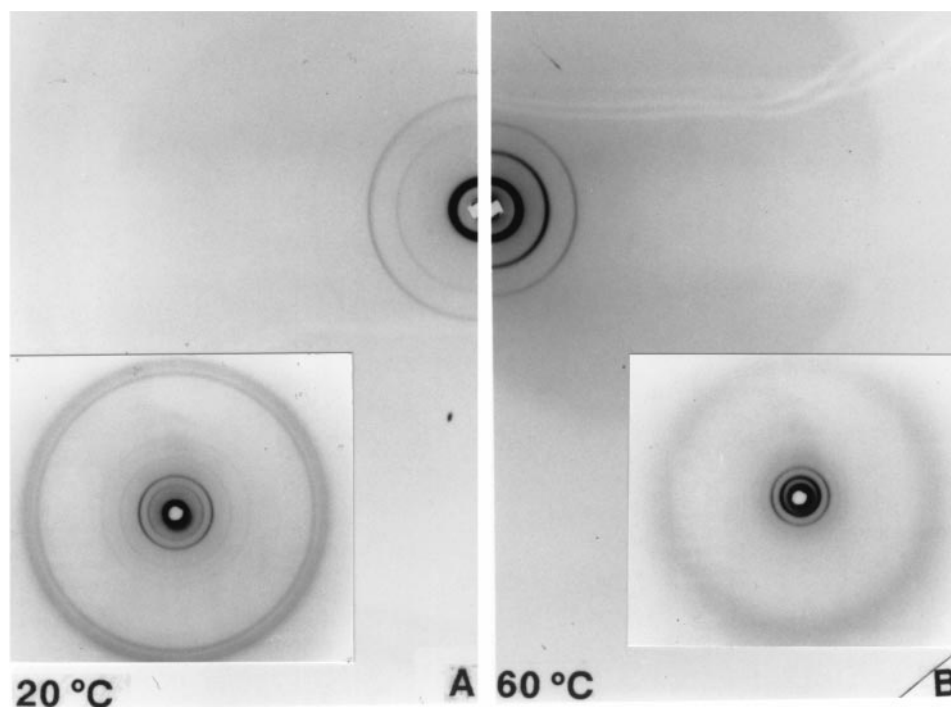
reflection is absent (see also Fig. 5 *A*). At 48°C, the diffraction pattern changes. The diffraction pattern of the 63-Å bilayer phase is still present, albeit weaker, together with two additional reflections at ~95 and ~48 Å. Above 48°C, three lamellar reflections indexing to a bilayer periodicity $d \approx 95$ Å are observed. Thus the data shown in Fig. 6 demonstrate clearly that C16:0-GalSulf at 60 wt% water

undergoes a bilayer transition at ~48°C, in good agreement with the DSC studies of C16:0-GalSulf in buffer (see Figs. 1–3).

The bilayer periodicity d of C16:0-GalSulf is plotted as a function of hydration (both as buffer and water) in Fig. 7. At 60°C, C16:0-GalSulf bilayers exhibit the continuous swelling behavior characteristic of charged lipids, with the bi-

FIGURE 5 X-ray diffraction patterns of hydrated (60 wt% water) C16:0-GalSulf, recorded with a Franks camera at (*A*) 20°C (below the chain-melting transition) and (*B*) 60°C (above the chain-melting transition). Corresponding x-ray diffraction patterns recorded with a toroidal camera are shown as insets (*left*, 20°C; *right*, 60°C).
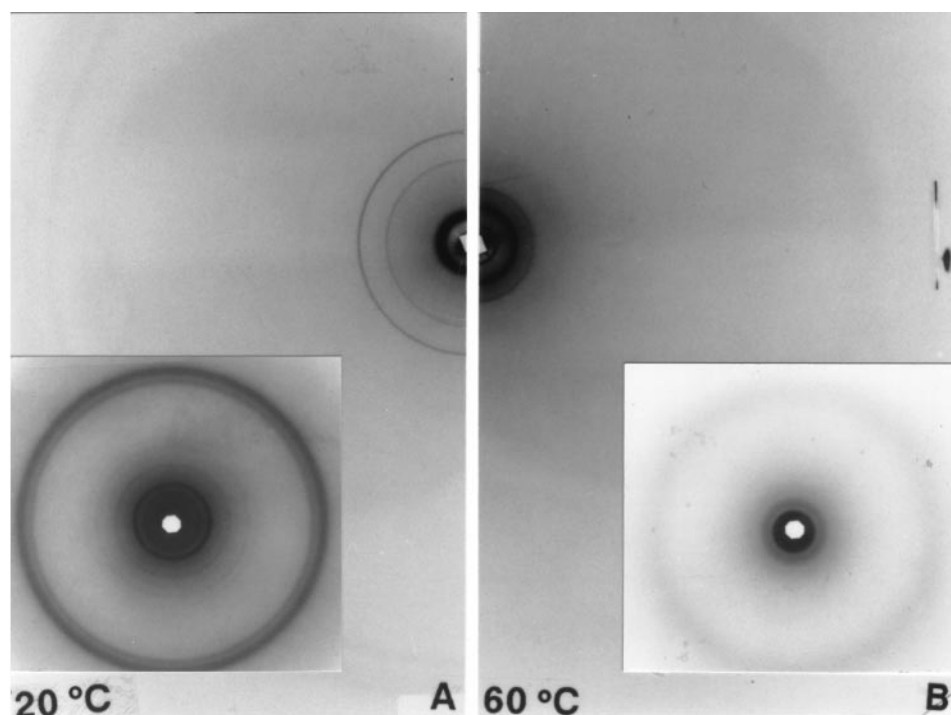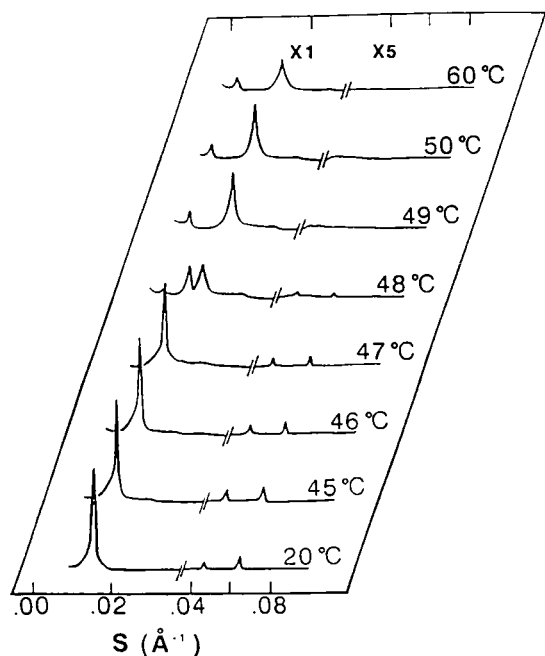
FIGURE 6 X-ray diffraction patterns, recorded with a linear position-sensitive detector, of hydrated (60 wt% water) C16:0-GalSulf at various temperatures.

layer periodicity increasing from 43.6 to 106.0 Å over the hydration range 0–62 wt% water/buffer. In contrast, at 20°C, a small increase (58.0 to 63.9 Å) in the bilayer periodicity d occurs between 0 and 15 wt% buffer, but at all higher hydrations (water or buffer) the bilayer periodicity of C16:0-GalSulf is essentially invariant ($d \approx 64$ Å). Thus the hydration/swelling characteristics of C16:0-GalSulf are different for the melted-chain L_α bilayer phase (continuous swelling) and the bilayer gel phase (limited hydration).
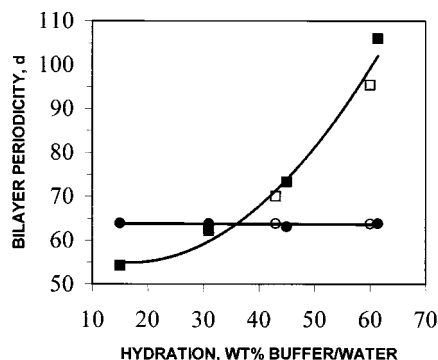

FIGURE 7 Bilayer periodicity (d) for C16:0-GalSulf/buffer and C16:0-GalSulf/water as a function of hydration (wt% water/buffer) at 20°C (●, buffer; ○, water) and 60°C (■, buffer; □, water) for hydrated samples and 95°C for anhydrous C16:0-GalSulf. Buffer: 50 mM sodium phosphate, pH 7.0; 50 mM NaCl.

Interestingly, for both the gel and L_α bilayer phases the swelling data for C16:0-GalSulf in buffer and water fall on the same lines (see Fig. 7). Apparently, the molarity of the buffer salts (50 mM sodium phosphate and 50 mM NaCl) is insufficient to affect the swelling properties of the NH_4^+ salt of C16:0-GalSulf in either of the bilayer phases.

DISCUSSION

As shown by DSC (see Figs. 1 and 2), aqueous dispersions of C16:0-GalSulf undergo a reversible gel → liquid-crystal chain-melting transition. Over the hydration range 0–19 wt% buffer the transition temperature decreases linearly from 93°C to 49°C (Fig. 3 A). The transition enthalpy and entropy increase over this hydration range, reaching limiting values of 8 kcal/mol and 165 cal/mol/°C, respectively, at ~19 wt% buffer (Fig. 3 B). It is worth noting that bovine brain sulfatide, despite a more complex fatty acid composition containing mainly longer chain fatty acids (particularly C24:0), has its major chain-melting transition at 47°C and a weaker transition at 35°C. Presumably in this case the chain-melting behavior reflects a balancing of the contributions of increased chain length and sulfatide molecular heterogeneity. In their systematic studies of sulfatides of different chain length in the range 16:0 to 24:0, Boggs and co-workers (Koshy and Boggs, 1983; Boggs et al., 1984) have shown that the chain-melting transition temperature increases with increasing chain length. For C16:0 sulfatide, Koshy and Boggs (1983) report a transition temperature $T_M = 50°C$ ($\Delta H = 8.5$ kcal/mol), in good agreement with the thermodynamic parameters reported here.

These thermodynamic parameters differ markedly from those exhibited by the corresponding C16:0 galactocerebroside, C16:0-GalCer. C16:0-GalCer exhibits a chain melting transition at 82°C (Ruocco et al., 1981) with corresponding changes in transition enthalpy ($\Delta H = 17.5$ kcal/mol) and entropy ($\Delta S = 213$ cal/mol/°C). Thus the introduction of the sulfate group at the 3-position of galactose leads to major reductions in the transition temperature (82 → 49°C), transition enthalpy (17.5 → 8 kcal/mol), and transition entropy (213 → 165 cal/mol/°C). In our earlier studies we have argued that high-temperature, high-enthalpy transition of C16:0-GalCer was due to the presence of both an ordered "crystalline chain" packing arrangement and an extensive intermolecular lateral hydrogen bonding network in its low-temperature bilayer phase (Ruocco et al., 1981). The x-ray diffraction pattern from this bilayer phase of C16:0-GalCer is characterized by multiple strong reflections in the wide-angle region (see figure 9b of Ruocco et al., 1981), indicative of "crystalline" chain and molecular packing. In contrast, the incorporation of the charged sulfate group in C16:0-GalSulf apparently precludes formation of this highly structured bilayer gel phase, as evidenced by a much simpler wide-angle diffraction pattern (see Figs. 4 A and 5 A). Presumably the charge characteristics of the sulfate

group lead to lateral charge-charge repulsion effects at the galactose sugar-interface region, thus prohibiting the formation of the highly ordered bilayer phase characteristic of C16:0-GalCer (Ruocco et al., 1981). Thus apparently the gel phase of C16:0-GalSulf is less ordered than that of C16:0-GalCer. In contrast, the lateral packing in the melted-chain L_α bilayer phase is presumably similar for C16:0-GalSulf and C16:0-GalCer, at least as evidenced by the similar broad diffraction at $\sim 1/4.5 \text{ Å}^{-1}$ (compare Figs. 4 B and 5 B with figure 9c of Ruocco et al., 1981). Presumably, the less ordered intermolecular and chain packing of the gel phase of C16:0-GalSulf compared to C16:0-GalCer results in a less stable gel phase that undergoes its transition to its L_α bilayer phase at a lower temperature and with a lower transition enthalpy and entropy.

In terms of structure, two key observations have been made, and they are summarized in Fig. 7. First, while the bilayer L_α phase at 60°C exhibits classical continuous swelling, the bilayer gel phase at 20°C shows only limited hydration behavior (see Fig. 7). Second, C16:0-GalSulf exhibits identical swelling when hydrated with either buffer or water; this is valid for both the bilayer gel and bilayer L_α phases (see Fig. 7). Introduction of the fully ionized sulfate group (Abramson et al., 1967) allows C16:0-GalSulf, in contrast to C16:0-GalCer (Ruocco et al., 1981; Saxena et al., 1999), to exhibit continuous bilayer swelling in the L_α phase, as all of the available water is incorporated between adjacent bilayers (see Fig. 7). Our previous studies of bovine brain sulfatide showed similar swelling behavior in its melted-chain bilayer phase (Ruocco and Shipley, 1986). This hydration behavior is observed for most anionic lipids and is attributable to charge-induced repulsion of bilayers. For example, charge-induced bilayer swelling has been observed for simple single-chain lipids (e.g., Na^+ and K^+ soaps; Luzzati et al., 1960) as well as the more complex anionic phospholipids (such as phosphatidylserine; Hauser et al., 1982). In most cases, the presence of a net charge at the bilayer surface results in continuous swelling behavior in both the melted-chain L_α phase and in the low-temperature bilayer gel phase. Notable exceptions to this rule appear to be the inability of C16:0-GalSulf (see above) and the Na^+, but not K^+, soaps (Luzzati et al., 1960; Vincent and Skoulios, 1966) to swell significantly in their respective bilayer gel phases. While a detailed molecular explanation for the different swelling behaviors in the gel and L_α bilayer phases of C16:0-GalSulf remains unclear, presumably the increased interfacial molecular area and resultant altered surface charge density that occurs on chain melting allow full expression of the interbilayer charge repulsion effects. However, in the low-temperature gel phase the galactosyl sulfate conformation and the interfacial packing (perhaps involving more extensive intermolecular H-bonding) must lead to a shielding of the sulfate negative charge and, at most, limited swelling results. Thus the limited hydration behavior of the charged C16:0-GalSulf in its gel phase is

quite similar to that of the uncharged C16:0-GalCer (Ruocco et al., 1981; Saxena et al., 1999).

Although we have emphasized the importance of the electrostatic charge repulsion force in producing bilayer swelling, other interbilayer forces can contribute to net bilayer repulsion. For example, the repulsive fluctuation force (Evans and Parsegian, 1986; Evans, 1991) may enhance bilayer repulsion, particularly in liquid-crystalline L_α phases. In the case of C16:0-GalSulf, the fully ionized state of sulfatide at pH 7 and its bilayer interfacial area per molecule of $\sim 60 \text{ Å}^2$ result in a high surface charge density; thus the electrostatic repulsive term is likely to be dominant in bilayer swelling. More puzzling is the failure of the bilayer gel phase of C16:0-GalSulf to undergo significant swelling. Since the interfacial area is smaller in the bilayer gel phase ($\sim 44 \text{ Å}^2$), the surface charge density is presumably higher in this phase than the L_α phase. While the nonelectrostatic repulsive fluctuation force is likely to be smaller in the gel phase, thus favoring nonswelling behavior, the electrostatic term in most cases appears to dominate. In a recent study, Kulkarni et al. (1999) showed that the nonswelling bovine brain GalCer gel phase could be induced to swell by incorporation of ≥ 17 mol % of a charged dipalmitoylphosphatidylglycerol into the bilayer. Thus increasing the surface charge density above a critical value leads to net bilayer electrostatic repulsion. In this context, it is not clear why the presumably higher surface charge density associated with the fully charged gel phase is insufficient to allow bilayer swelling of C16:0-GalSulf. Perhaps for the bovine brain GalCer gel phase the addition of dipalmitoylphosphatidylglycerol contributes both an electrostatic repulsive force and, at the same time, disrupts both lateral intrabilayer and interbilayer attractive forces. Clearly, this would not be the case for C16:0-GalSulf. We also note that a much earlier study showed that a sulfated algal glycolipid, sulfoquinovosyl diglyceride, demonstrated temperature-dependent swelling behavior: limited swelling in its gel phase and continuous swelling in the L_α phase (Shipley et al., 1973).

In summary, the presence of the charged sulfate group at the 3-position of the galactose group of C16:0-GalSulf leads to a significant reduction in the chain-melting temperature, enthalpy, and entropy compared to C16:0-GalCer. Predictably, the charged sulfatide exhibits continuous swelling in its bilayer L_α phase; somewhat surprisingly, the charge-mediated bilayer repulsion effects are muted in the bilayer gel phase (Fig. 7). Thus C16:0-GalSulf exhibits a chain-melting transition at 49°C, a transition at which major changes in both hydrocarbon chain packing and interbilayer hydration occur.

REFERENCES

Abrahamsson, S., I. Pascher, K. Larsson, and K.-A. Karlsson. 1972. Molecular arrangements in glycosphingolipids. *Chem. Phys. Lipids.* 8:152–179.

Abramson, M. B., R. Katzman, R. Curci, and C. E. Wison. 1967. The reactions of sulfatide with metallic cations in aqueous systems. *Biochemistry.* 6:295–304.

Berridge, M. J. 1993. Inositol triphosphate and calcium signalling. *Nature.* 361:315–325.

Bitman, J., and D. L. Wood. 1982. An improved copper reagent for quantitative densitometric thin-layer chromatography of lipids. *J. Liq. Chromatogr.* 5:1155–1162.

Boggs, J. M., K. M. Koshy, and G. Rangaraj. 1984. Effect of fatty acid chain length, fatty acid hydroxylation, and various cations on phase behavior of synthetic cerebroside sulfate. *Chem. Phys. Lipids.* 36:65–89.

Boggs, J. M., K. M. Koshy, and G. Rangaraj. 1988a. Influence of structural modifications on the phase behavior of semi-synthetic cerebroside sulfate. *Biochim. Biophys. Acta.* 938:361–372.

Boggs, J. M., K. M. Koshy, and G. Rangaraj. 1988b. Interdigitated lipid bilayers of long acyl chain species of cerebroside sulfate. A fatty acid spin label study. *Biochim. Biophys. Acta.* 938:373–385.

Brown, D. A., and E. London. 1998. Functions of lipid rafts in biological membranes. *Annu. Rev. Cell Dev. Biol.* 14:111–136.

Curatolo, W. 1982. Thermal behavior of fractionated and unfractionated bovine brain cerebrosides. *Biochemistry.* 21:1761–1764.

Curatolo, W., D. M. Small, and G. G. Shipley. 1977. Phase behavior and structural characteristics of hydrated bovine brain gangliosides. *Biochim. Biophys. Acta.* 468:11–20.

Elliot, A. J. 1965. The use of toroidal reflecting surfaces in x-ray diffraction cameras. *J. Sci. Instrum.* 42:312–316.

Evans, E. 1991. Entropy-driven tension in vesicle membranes and unbinding of adherent vesicles. *Langmuir.* 7:1900–1908.

Evans, E. A., and V. A. Parsegian. 1986. Thermal-mechanical fluctuations enhance repulsion between bimolecular layers. *Proc. Natl. Acad. Sci. USA.* 83:7132–7136.

Exton, J. H. 1994. Messenger molecules derived from membrane lipids. *Curr. Opin. Cell Biol.* 6:226–229.

Fishman, P. H., T. Pacuszka, and P. A. Orlandi. 1993. Gangliosides as receptors for bacterial enterotoxins. *Adv. Lipid Res.* 25:165–187.

Franks, A. 1958. Some developments and applications of microfocus x-ray diffraction techniques. *Br. J. Appl. Phys.* 9:349–352.

Ginsburg, V., and D. D. Roberts. 1988. Glycoconjugates and cell adhesion: the adhesive proteins laminin, thrombospondin and von Willebrand's factor bind specifically to sulfated glycolipids. *Biochimie.* 70:1651–1659.

Haas, N. S., and G. G. Shipley. 1995. Structure and properties of N-palmitoyleoyl-galactosyl-sphingosine (cerebroside). *Biochim. Biophys. Acta.* 1240:133–141.

Hakomori, S., and Y. Igarashi. 1995. Functional role of glycosphingolipids in cell recognition and signaling. *J. Biochem.* 118:1091–1103.

Hannun, Y. A. 1994. Sphingomyelin cycle and the second messenger function of ceramide. *J. Biol. Chem.* 269:3125–3128.

Harouse, J. M., S. Bhat, S. L. Spitalnik, M. Laughlin, K. Stefano, D. H. Silberberg, and F. Gonzalez-Scarano. 1991. Inhibition of entry of HIV-1 in neural cell lines by antibodies against galactosyl ceramide. *Science.* 253:320–323.

Hauser, H., F. Paltauf, and G. G. Shipley. 1982. Structure and thermotropic properties of phosphatidylserine bilayer membranes. *Biochemistry.* 21:1061–1067.

Koshy, K. M., and J. M. Boggs. 1982. A high-yield saponification of galactosylceramide I³-sulfate. *Lipids.* 17:998–1000.

Koshy, K. M., and J. M. Boggs. 1983. Partial synthesis and physical properties of cerebroside sulfate containing palmitic acid or α-hydroxy palmitic acid. *Chem. Phys. Lipids.* 34:41–53.

Kulkarni, K., D. S. Snyder, and T. J. McIntosh. 1999. Adhesion between cerebroside bilayers. *Biochemistry.* 38:15264–15271.

Luzzati, V. 1968. X-ray diffraction studies of lipid-water systems. *In* Biological Membranes, Vol. 1. D. Chapman, editor. Academic Press, New York. 71–123.

Luzzati, V., H. Mustacchi, A. Skoulios, and F. Husson. 1960. La structure des colloides d'association. I. Les phases liquide-cristallines des systemes amphiphile-eau. *Acta Crystallogr.* 13:660–667.

Lynch, D. V., M. Caffrey, J. L. Hogan, and P. L. Steponkus. 1992. Calorimetric and x-ray diffraction studies of rye glucocerebroside. *Biophys. J.* 61:1289–1300.

Marchesini, S., P. Viani, G. Cervato, D. Monti, B. Cestaro, and C. Oliva. 1987. Preparation of spin-labelled sulfatides for EPR studies on model membranes. *Biochem. Int.* 14:491–499.

Marinier, A., A. Martel, J. Banville, C. Bachand, R. Remillard, P. Lapointe, B. Turmel, M. Menard, W. E. Harte, Jr., J. J. K. Wright, G. Todderud, K. M. Tramposch, J. Bajorath, D. Hollenbaugh, and A. Aruffo. 1997. Sulfated galactocerebrosides as potential antiinflammatory agents. *J. Med. Chem.* 40:3234–3247.

Nishizuka, Y. 1992. Intracellular signaling by hydrolysis of phospholipids and activation of protein kinase C. *Science.* 258:607–614.

Nonaka, G., Y. Kishimoto, Y. Seyama, and T. Yamakawa. 1979. Formation of lysosulfatide, 3′,6′-anhydropsychosine, ceramide, and sphingosine by saponification of cerebroside sulfate. Effect of the sulfate group on the hydrolysis. *J. Biochem.* 85:511–518.

Reed, R. A., and G. G. Shipley. 1987. Structure and metastability of N-lignoceryl-galactosylsphingosine (cerebroside) bilayers. *Biochim. Biophys. Acta.* 896:153–164.

Reed, R. A., and G. G. Shipley. 1989. Effect of chain unsaturation on the structure and thermotropic properties of galactocerebrosides. *Biophys. J.* 55:281–292.

Reiss-Husson, F. 1967. Structure des phases liquide-cristalline de differents phospholipides, monoglycerides, sphingolipides, anhydres ou en presence d'eau. *J. Mol. Biol.* 25:363–382.

Roberts, D. D. 1986. Sulfatide-binding proteins. *Chem. Phys. Lipids.* 42:173–183.

Ruocco, M. J., D. Atkinson, D. M. Small, R. P. Skarjune, E. Oldfield, and G. G. Shipley. 1981. X-ray diffraction and calorimetric study of anhydrous and hydrated N-palmitoylgalactosylsphingosine (cerebroside). *Biochemistry.* 20:5957–5966.

Ruocco, M. J., and G. G. Shipley. 1983. Hydration of N-palmitoylgalactosylsphingosine compared to monosaccharide hydration. *Biochim. Biophys. Acta.* 735:305–308.

Ruocco, M. J., and G. G. Shipley. 1984. Interaction of cholesterol with galactocerebroside and galactocerebroside-phosphatidylcholine bilayer membranes. *Biophys. J.* 46:695–707.

Ruocco, M. J., and G. G. Shipley. 1986. Thermal and structural behavior of natural cerebroside 3-sulfate in bilayer membranes. *Biochim. Biophys. Acta.* 859:246–256.

Ruocco, M. J., G. G. Shipley, and E. Oldfield. 1983. Galactocerebroside phospholipid interactions in bilayer membranes. *Biophys. J.* 43:91–101.

Saxena, K., R. I. Duclos, P. Zimmermann, R. R. Schmidt, and G. G. Shipley. 1999. Structure and properties of totally synthetic galacto- and gluco-cerebrosides. *J. Lipid Res.* 40:839–849.

Saxena, K., P. Zimmermann, R. R. Schmidt, and G. G. Shipley. 2000. Bilayer properties of totally synthetic C16:0-lactosyl-ceramide. *Biophys. J.* 78:306–312.

Shah, J., J. M. Atienza, R. I. Duclos, A. V. Rawlings, Z. Dong, and G. G. Shipley. 1995. Physical properties of ceramides: effect of fatty acid hydroxylation. *J. Lipid Res.* 36:1936–1944.

Shipley, G. G., J. P. Green, and B. W. Nichols. 1973. The phase behavior of monogalactosyl, digalactosyl, and sulphoquinovosyl diglycerides. *Biochim. Biophys. Acta.* 311:531–544.

Suzuki, Y., Y. Toda, T. Tamatani, T. Watanabe, T. Suzuki, T. Nakao, K. Murase, M. Kiso, A. Hasegawa, K. Tadano-Aritomi, I. Ishizuka, and M. Miyasaka. 1993. Sulfated glycolipids are ligands for a lymphocyte homing receptor, L-selectin (LECAM-1), binding epitope in sulfated sugar chain. *Biochem. Biophys. Res. Commun.* 190:426–434.

Taketomi, T., A. Hara, Y. Kutsukake, and E. Sugiyama. 1990. New approach for characterization of lysosulfatide by TLC, fast atom bombardment mass spectrometry and NMR spectroscopy. *J. Biochem.* 107: 680–684.

Tanahashi, E., K. Murase, M. Shibuya, Y. Igarashi, H. Ishida, A. Hasegawa, and M. Kiso. 1997. Synthetic studies on selectin ligands/ inhibitors: a systematic synthesis of sulfatide and its higher congeners carrying 2-(tetradecyl)hexadecyl group as a ceramide substitute. *J. Carbohydr. Chem.* 16:831–858.

van den Berg, L. H., S. A. Sadiq, S. Lederman, and N. Latov. 1992. The gp120 glycoprotein of HIV-1 binds to sulfatide and to the myelin associated glycoprotein. *J. Neurosci. Res.* 33:513–518.

Vincent, J. M., and A. Skoulios. 1966. Gel et coagel. I. Identification. Localisation dans un diagramme de phases et determination de la structure du gel dans le cas du stearate de potassium. *Acta Crystallogr.* 20:432–440.